COLLISIONS OF $\lesssim$1 BEV PARTICLES (EXCLUDING ELECTRONS AND PHOTONS) WITH NUCLEI[1]

By S. J. Lindenbaum
Brookhaven National Laboratory, Long Island, N. Y.

Introduction

In the past several years a great deal of progress has been made in experimentally determining the properties of the collisions of particles exhibiting strong nuclear interactions both with each other and with nuclei. Pions[2] and nucleons have been most extensively studied. Their relatively long lifetime and abundant production at various accelerators have provided beams of these particles of sufficient intensity for detailed observation of the interactions resulting from their collisions with nculeons and nuclei.

The greatest theoretical attack has been made on pion-nucleon interactions. It has been particularly encouraging that most of the dominant features of the lower energy interactions (pions of kinetic energy <250 Mev) have been satisfactorily explained by one resonant state of isotopic spin (T) and angular momentum (J) equal to 3/2, with a resonant energy of $\sim$190 Mev (kinetic—L.S.) and the considerable peak cross-section of about 200 mb (millibarns) near the resonance.

The higher energy pion-nucleon interactions (500 Mev to $\gtrsim$1 Bev) are less understood; however, one dominant feature is that the $T=\frac{1}{2}$ cross-section has a peak of $\sim$60 (mb) at about 1 Bev while the $T=3/2$ cross-section is generally much smaller in this region. However, it has a rise from a minimum of $\sim$15 mb near 650 Mev to a peak of $\sim$40 mb near 1.3 Bev.

The concept of charge independence or conservation of isotopic spin in strong nuclear interactions has been successfully applied in analyzing the data, and has not been contradicted in any experiment performed to date. Elastic nucleon-nucleon collisions below 500 Mev are still only partially understood; however, the behavior of the cross-sections experimentally is quite well known. Above 500 Mev, pion production becomes important and the properties of the pion-nucleon interaction seem to play a predominant role in this. The total p-p and n-p cross-sections and the elastic and inelastic parts of the p-p cross-section have been fairly well determined. The elastic

[1] The general survey of literature pertaining to this review was completed in December, 1956. However, some particularly relevant later publications previously available privately to the author have been referred to.

[2] The term pion for the π-meson has been extensively employed lately and will be used freely throughout this article. Energies cited will be kinetic energy in the lab system unless otherwise specified.

cross-section at these higher energies can be generally explained as a diffraction cross-section accompanying the inelastic meson production.

The interactions of nucleons with nuclei (kinetic energy $\gtrsim$50 Mev) is generally consistent with the optical model, and the inelastic parts thereof can be explained in terms of primary nucleon-nucleon encounters in the nucleus which are followed by a nucleonic cascade of the nucleons and produced pions, and finally by an evaporation process.

The interactions of pions with nuclei are generally consistent with primary pion encounters with one or a pair of nucleons in nuclear matter followed by nucleonic cascade initiated by the products which often includes absorption of the pion and finally an evaporation process.

The treatment in this article will be confined exclusively to those particles produced prolifically in collisions of $\lesssim$1 Bev nucleons with nuclei, namely nucleons and pions. The major emphasis will be placed on those interactions of pions and nucleons with nucleons and nuclei, which are important for incident energy of $\lesssim$1 Bev. However, the treatment will be extended to higher energies in cases such as pion production and pion interactions, where the physical phenomenon is either essentially clarified thereby, or relevant individual investigations considered have extended to higher energies.

The cross-section for the production of strange particles is less than $\sim$3 per cent of the inelastic cross-section in all collisions considered here. Strange particle production and interactions will be reviewed in this volume by Gell-Mann & Rosenfeld in an article entitled "Hyperons and Heavy Mesons (Systematics and Decay)" (cf. p. 407). Therefore these subjects will not be considered here.

It is clear that all relevant topics in pion snd nucleon collisions cannot be fully treated in this review and that some will have to be omitted or mentioned briefly.

Collisions of Positive and Negative Pions with Hydrogen

The scattering of $\pi^{\pm}$ mesons by hydrogen.—Since the previous review by Gell-Mann & Watson (1) three years ago, the available data on the total and differential cross-section of $\pi^+ + p$ have increased markedly both in the number of measurements and the accuracy thereof. Figure 1 shows a compilation of the latest and most accurate available data on the $\pi^+ + p$ total cross-section for incident pion energies of 125 to 250 Mev. The $\pi^+ + p$ scattering for this energy region has received a great deal of attention lately, since it involves a pure isotopic spin 3/2 state, and hence is best suited for determining whether there is, as now generally believed, a resonance in the state of isotopic spin and angular momentum 3/2 at a pion kinetic energy of $\sim$190 Mev. The most extensive investigations have been made by Ashkin *et al.* (2), Lindenbaum & Yuan (3, 4), and Mukhin *et al.* (5, 6). The absolute accuracy of the behavior of these total cross-sections as a function of energy is now generally known within $\pm$5 per cent, and the relative value of the

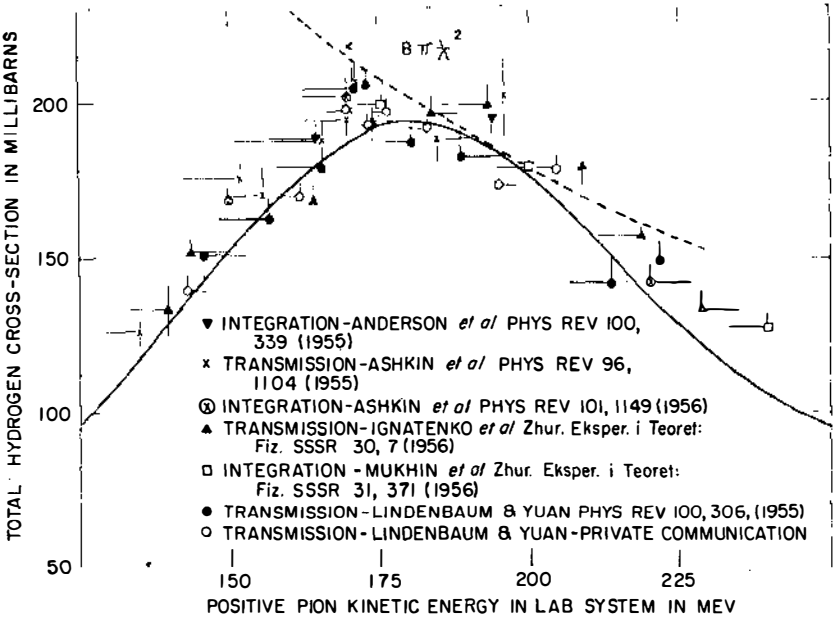

FIG. 1. A plot of the latest and most accurate $\pi^+ + p$ total cross-section data in the energy region 125 to 250 Mev. The solid line represents the contribution of α_{33} alone, taken from Fig. 2 (2 to 6, 10, 11).

$\pi^+ + p$ total cross-section curve around the resonance peak has now been determined to approximately ± 2 per cent in a recent experiment (4).

The $8\pi\lambda\!\!\!^{-2}$ curve shows the contribution to the $\pi^+ + p$ total cross-section at the resonance energy, due to a P-wave resonance in the state of isotopic spin (T) and angular momentum (J) equal to 3/2. It is clear that within the errors the total $\pi^+ + p$ cross-section curve appears to be either tangent to or larger than the $8\pi\lambda\!\!\!^{-2}$ line in the region of 180 to 200 Mev. Hence these data are consistent with a resonance in the $T = J = 3/2$ state in this energy region.

The Chew-Low equation.—Chew & Low (7b) recently investigated an exact equation deduced by Low (7a) for pion-nucleon interactions which included the pion cloud effects in the nuclear wave function and obtained as an approximate solution for the scattering in the symmetric pseudoscalar meson theory in the one meson approximation:

$$\frac{\eta^3}{\omega_t^*} \cot \alpha_{33} = \frac{3}{4} (f^2)^{-1} F(\omega_t^*) \qquad 1.$$

Where η is the c.m.s. pion momentum in units of $m_\pi c$; ω_t^* is the total c.m.s. energy of the pion plus the nucleon kinetic energy[3] in units of $m_\pi c^2$; m_π is the pion rest mass; c is the velocity of light; α_{33} is the phase shift in the $T = J = 3/2$

[3] The inclusion of the recoil nucleon kinetic energy in the total c.m.s. energy (π_t^*) is an attempt to take into account approximately the nucleon recoil effects.

state; f^2 is the renormalized unrationalized coupling constant; and $F(\omega_t^*)$ is of the form $1-\omega_t^* r_a(\omega_t)^*$ with $r_a(\omega_t^*)$ almost a constant for small ω_t^*. This allows a determination of f^2 by extrapolation as will be explained later.

Serber & Lee (c.f. p. 457 of ref. 9) have found that the exact solution of the Chew-Low equation for charged and neutral scalar meson theories in the one meson approximation is:

$$\frac{\eta^3}{\omega_t^*}\cot\alpha_{33} - \frac{1}{\omega_t^*} = \frac{3}{4}(f^2)^{-1}F(\omega_t^*) \qquad 2.$$

An analysis of the effective range approximation, the experimental data, and other reasons led Chew and Low to originally assume that $F(\omega_t^*)=1-(\omega_t^*/\omega_0^*)$ where ω_0^* is the resonance energy. One should note that the cut-off model (7b) predicts a low energy resonance in the $T=J=3/2$ state for the observed values of the coupling constant, provided that the cut-off energy ω_{max} is large enough. The resonance energy (ω_0) depends on f^2 and ω_{max}, and therefore ω_0 can replace ω_{max} as a parameter in the theory. It has been shown (3) that this particular choice (Eq. 2) for $F(\omega_t^*)$ results in a variation of the $\pi^+ + p$ total cross-section generally similar to the one obtained by Brueckner (8), when he fitted a one-level Breit-Wigner resonance formula to the observed energy variation of the $\pi^+ + p$ total cross-section assuming the $T=J=3/2$ state resonates.

It is also clear that with $F(\omega_t^*)=1-(\omega_t^*/\omega_0^*)$, if the left hand side of Eqs. 1 or 2 is plotted as an ordinate, versus ω_t^* as an abcissa, a straight line is predicted by the theory which determines the resonance energy at the point where $\cot\alpha_{33}=0$. This is the point where the ordinate is 0 or $-(1/\omega_t^*)$, for the Chew-Low plot or Serber-Lee plot, respectively. The coupling constant f^2 is also obtained by extrapolating the line to determine the y intercept at $\omega_t^*=0$.[4]

The Serber-Lee plot is shown in Figure 2. The values of α_{33} were obtained from the best values of the phase shift analysis of the differential scattering and charge exchange cross-section of pion-nucleon scattering. These experiments will be discussed later.

It is clear from Figure 2 that the data can be fitted by one straight line below resonance and another straight line of considerably different slope above resonance. This change in slope exists also for the Chew-Low plot (not shown) as well as for the Serber-Lee plot and has been previously suggested (3).

The resonance energy is defined as that energy where α_{33} passes through 90° or equivalently where the ordinate of the Serber-Lee plot equals $-(1/\omega_t^*)$. Due to the change in slope of the Serber-Lee plot near resonance,

[4] Chew & Low (7b) point out that the change in f^2 due to the inclusion the $-(1\omega_t^*)$ term in the ordinate of the plot may be of the same order of magnitude as the second order correction and the errors in the experimental data.

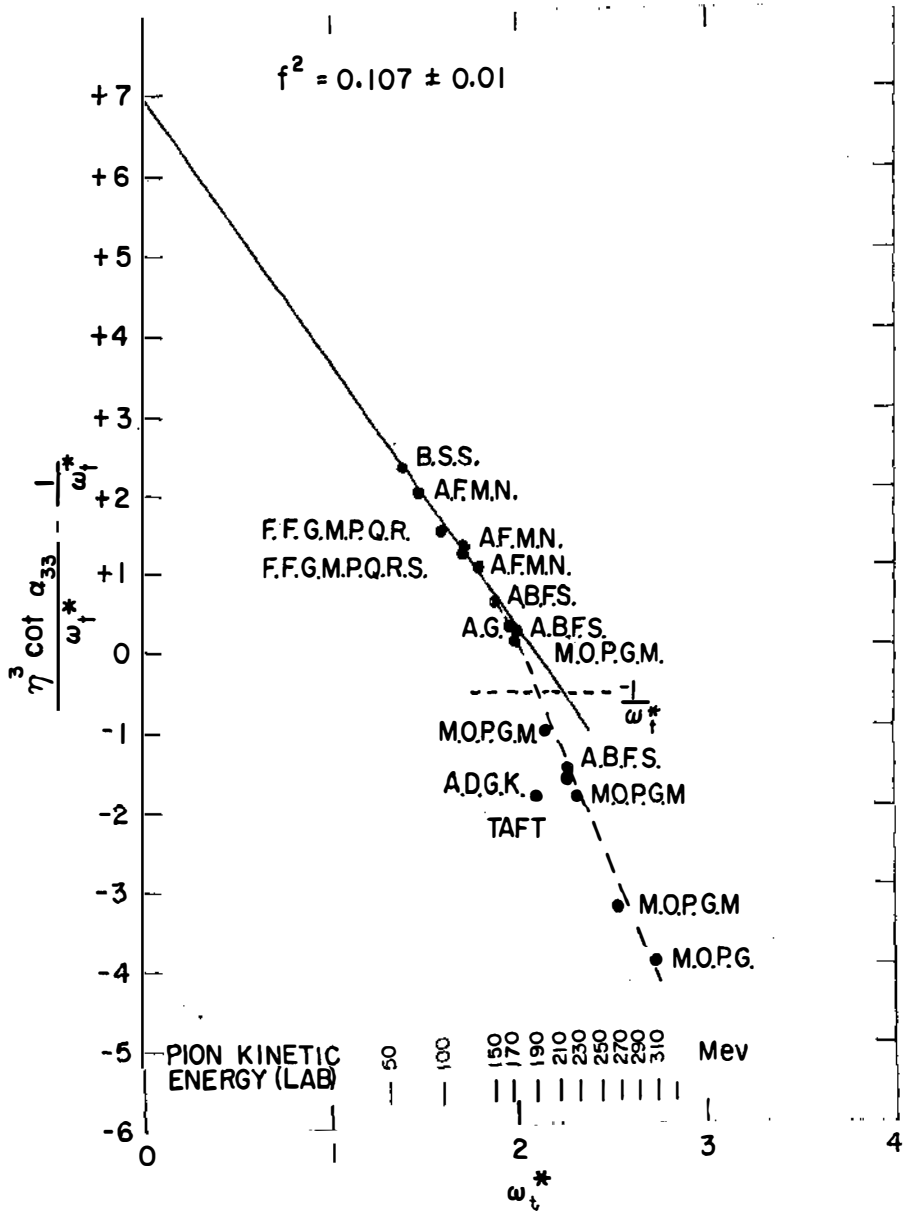

FIG. 2. A Serber-Lee plot—see text on original Chew-Low plot which is similar except for lack of $-(1/\omega_t^*)$ term in the ordinate. Initials of author's last names are used for identification of points (6, 10, 11, 12, 16, 17, 27).

the intersection of the plot with the $-(1/\omega_t^*)$ curve is uncertain. However the best guess for which the rate of change in slope is not too rapid, is that the intersection of the broken line (solution above resonance) with the $-(1/\omega_t^*)$ curve is the resonant point. A reasonable estimate from Figure 2 is that the resonant energy is 190_{-10}^{+20} Mev, where the estimation of errors is somewhat arbitrary and uncertain.

The fact that the Serber-Lee or Chew-Low plots are not unique straight lines is not surprising, since $F(\omega_t^*)$ was more or less arbitrarily chosen and its form can only be even approximately justified near $\omega_t^* \simeq 1$. One might also note that the resonance energy is approximately at the threshold for producing an additional pion; hence two meson states may begin to contribute appreciably. Furthermore, Castillejo *et al.* (9) have investigated the Chew-Low equation for charged and neutral scalar meson theories treated in the one meson approximation. They demonstrated that the Chew-Low equation does not have a unique solution, and indeed does not contain more information or restrictions than a generalized dispersion formula of the Wigner-Eisenbud type. It is not at present known whether this also holds true for pseudoscalar meson theory when all higher approximations are included, however, there is certainly no reason to assume that a unique and more restrictive solution exists for the pseudoscalar case. It was previously pointed out (3), that the particular solutions chosen by Chew & Low and Serber & Lee have properties generally similar to a P-wave Breit-Wigner one-level resonance formula plotted in a linear form, and hence represent convenient ways to analyze the data. Furthermore, Chew & Low point out that their solution may possibly be the only one of physical interest.[5]

The coupling constant deduced from Figure 2 is $f^2 = 0.107 \pm 0.01$. This value will be compared to others obtained by different methods in a subsequent section.

The contribution to the $\pi^+ + p$ total cross-section as a function of energy by the α_{33} phase shift variation is shown in Figure 1 and also Figure 3 where the solid line $\pi^+ + p$ curve has been computed this way until 650 Mev. The variation of α_{33} with energy was taken from the Serber-Lee plot (Fig. 2) by following the solid line to $\sim$170 Mev and the broken line thereafter. As one can see, the observed $\pi^+ + p$ total cross-section can be represented very well, to within a few per cent, by the contribution of α_{33} alone to energies well beyond the highest energy (307 Mev), for which α_{33} has been well determined. This curve has a peak in the laboratory system at a pion kinetic energy $\sim$180 Mev, and is consistent with a resonance in the $T = J = 3/2$ state at $\sim$190 Mev.

[5] Chew & Low (7b) point out that their solution is the only one which is an analytic continuation of the perturbation theory power series solution. Hence they argue if one assumes that the original field theoretic problem has a unique solution which is an analytic continuation of the power series then their solution is the only one of physical interest.

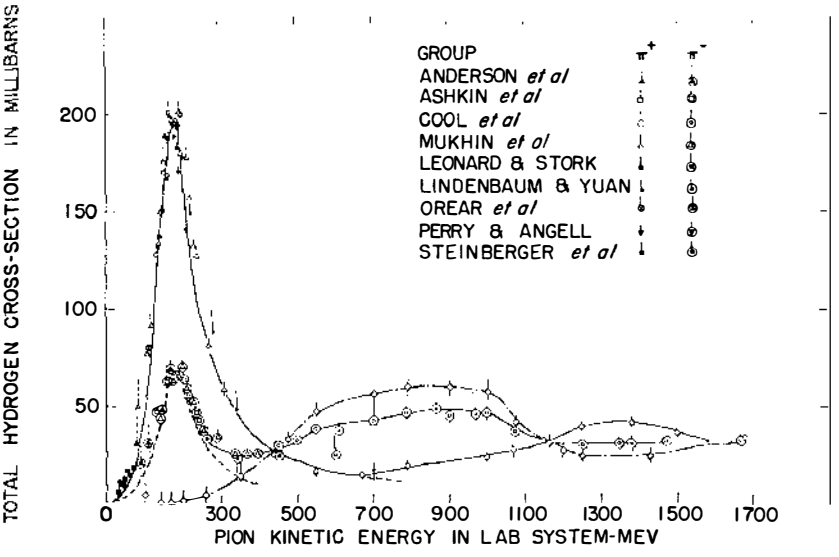

FIG. 3. A plot of $\pi^{\pm}+p$ total cross-sections as a function of energy, using in general significantly more accurate data when a choice exists. The contribution of α_{33} alone to the cross-section is shown for $\pi^{+}+p$ by the solid line below ~650 Mev and the broken line thereafter; for $\pi^{-}+p$ by the broken line. The following are empirical curves: the solid line for $\pi^{+}+p$ beyond ~650 Mev; the solid line for $\pi^{-}+p$; the dash-dot curve through the open diamond points was obtained for the $T=\frac{1}{2}$ cross-section by the standard subtraction method (2 to 6, 10, 11, 12, 15, 22, 25 to 28).

The phase shifts of the other S and P states namely α_3 and α_{31} which accompany the α_{33} resonance-solution are quite small and contribute $\lesssim$5 per cent to the $\pi^{+}+p$ total cross-section. These will be discussed in a later section. The contributions to the $\pi^{-}+p$ total cross-section as a function of energy by the α_{33} phase shift is shown in Figure 3 by the dashed line near the $\pi^{-}+p$ points. It is clear that up to ~200 Mev the total $\pi^{-}+p$ cross-section curve can be represented well, to within a few per cent, by the contribution of α_{33} alone.

One should note here that the extrapolation beyond 307 Mev of the line in the Serber-Lee plot which fits the data above resonance, is at best a questionable procedure since there are no accurate measurements of α_{33} beyond this energy. The apparent agreement of the $\pi^{+}+p$ total cross-section with this extrapolation to beyond 600 Mev may well be purely accidental. It will be pointed out later that even at 307 Mev there is some evidence that suggests an appreciable D-wave contribution which could of course become large at the higher energies.

Phase shifts.—The angular distribution of positive and negative pions incident on hydrogen which are direct and charge exchange scattered have

been extensively studied recently. The most extensive investigations have been performed by Ashkin *et al.* (10) for $\pi^{\pm}+p$ at 150, 170 and 220 Mev, Mukhin *et al.* (6) for $\pi^{+}+p$ at 176, 200, 240, 270 and 307 Mev,[6] and Anderson *et al.* (11) for $\pi^{\pm}+p$ at 165 and $\pi^{+}+p$ at 189 Mev. These results have been subjected to the S and P wave phase shift analysis first introduced by Fermi and his co-workers (12) which assumes charge independence and involves the six phase shifts α_3, α_{31}, α_{33}, α_1, α_{11}, and α_{13}. The first index equals twice the isotopic spin and the second equals twice the angular momentum. Although several possible solutions can be found to the data (13, 14), the one generally accepted as most likely to be physically significant and most compatible with all experimental observations is the Bethe-DeHoffman *et al.* (13a, 14) solution for the so-called Fermi phase shifts. In this solution α_{33} passes through resonance at about 195 Mev, and all others are small below 200 Mev.

A compilation of α_{33} phase shifts of this type are shown in Figure 2 in the form of the Serber-Lee plot. The sign of α_{33} has been determined by Orear (15), Ferrari *et al.* (16), and Taft (17) who observed the interference of $\pi^{+}+p$ nuclear scattering with the Coulomb scattering. This also determines the absolute sign of other phase shifts in a particular phase shift analysis. The values of α_3 appear to be consistent with the Orear proposal (18) $\alpha_3 = -0.11\eta$ until 200 Mev. Above 200 Mev α_3 seems to increase more rapidly with increasing η than the foregoing if only an S-P analysis is considered (6). However, under an S-P-D analysis (6) the foregoing prescription still seems to hold with small amounts of D wave predicted, namely:

$$\delta_{33} = +0.20^{0}\eta^{5} \quad \text{and} \quad \delta_{33} = -0.21^{0}\eta^{5}$$

These D wave formulae correspond to less than $\sim 10^{\circ}$ D-wave at 307 Mev, which is the highest energy analyzed.

The behavior of α_1 is less well known. However, the Orear prescription (18) of $\alpha_1 = 0.16\eta$ still seems consistent with the data.

The behavior of α_{31} is still uncertain. However, the analyses of recent $\pi^{+}+p$ differential cross-section experiments by Ferrari *et al.* (16) between 70 and 130 Mev and Mukhin *et al.* (6) between 176 and 307 Mev, make it appear likely that it is small and negative with a value of $\lesssim 10^{\circ}$ for energies below 307 Mev. The values of α_{13} and α_{11} are both small and essentially undetermined even by the latest analyses.

The other set of phase shifts which is of most interest is the Yang set (19) which is related to the Fermi or Bethe-deHoffmann set by the following equations:

$$\alpha_{33} - \alpha_{31} = -(\alpha_{33}' - \alpha_{31}') \qquad 3.$$

$$2e^{2i\alpha_{33}} + e^{2i\alpha_{31}} = 2e^{2i\alpha_{33}'} + e^{2i\alpha_{31}'} \qquad 4.$$

[6] Some work of lower statistical accuracies on positive pion scattering by hydrogen at 260, 300, and 400 Mev observed in hydrogen diffusion chambers has been reported by Margulies (89).

The Yang set has been found by Bethe & DeHoffman (13a, 14) to show three resonances ($\alpha_{31} = 90°$ and $270°$; $\alpha_{33} = 90°$) by the time the α_{33} of the Fermi solution has reached only 120°. This is considered to be a less likely physical behavior.

Another ambiguity in the phase shifts has been pointed out by Minami (20a), however, for several reasons [see p. 75 of ref. (14)] this solution is considered to be unlikely.

A recent application of causality using spin-flip amplitudes (21) supports the Fermi set and tends to reject the Yang set. An earlier different application of causality using non-flip amplitudes (22) could not rule out the Yang set.

Fermi pointed out that the polarization (23) of the recoil nucleon in meson-nucleon scattering is quite different for the Fermi and Yang phase shifts. Several experiments (24) are now in progress which are attempting to observe the polarization and so distinguish between the two sets on a direct absolute basis.

Hayakawa *et al.* (20b) have shown that the Minami ambiguity can also be settled by observing the polarization of the recoil nucleon.

Total $\pi^{\pm} + p$ cross-sections.—The total cross-section (2 to 6, 10 to 12, 15 to 18, 22, 25 to 28) of $\pi^{\pm} + p$ as a function of pion kinetic energy are plotted in Figure 3 (also see Fig. 1). The higher energy points have been mainly investigated by Cool, Piccioni & Clark (25). The assumption of charge independence, or, equivalently, conservation of isotopic spin, has been made in obtaining the total cross-sections for the two isotopic spin states $T = \frac{1}{2}$ and $T = 3/2$ which are involved in these interactions. The relations used are:

$$\sigma(\pi^+ + p) = \sigma(T = 3/2) \qquad 5.$$

$$\sigma(\pi^- + p) = \tfrac{1}{3}\sigma(T = 3/2) + 2/3\sigma(T = \tfrac{1}{2}) \qquad 6.$$

Since within the errors the $T = \frac{1}{2}$ cross-section is zero below 200 Mev it is implied that the low energy $\pi^- + p$ cross-section is probably mainly due to the previously noted resonance in the $T = J = 3/2$ state. In fact, the dashed line curve shows the total cross-section contribution computed from the α_{33} phase shift. The fit to the observed total cross-section is reasonably good to within a few per cent below 200 Mev. However the $T = \frac{1}{2}$ cross-section rises steeply above 200 Mev and reaches a peak at about 1.0 Bev. This phenomenon has been subjected to many investigations. One early proposal due to Dyson (29), Takeda (30), and Piccioni[7] (25) was that the 1.0 Bev peak is due to a resonance in the interaction of the incident pion with a pion in the nucleon cloud. This possibility has been investigated by several groups recently and does not appear to be consistent with the experimental data. One major difficulty is that the expected internal momentum distribution of the pion in the cloud would spread even a sharp resonance by

[7] A resonance corresponding to $J = 5/2$ has also been found to be compatible with the data by this group.

± 1 Bev/c (25) which would wash out the peaked behavior observed in the cross-section. Another difficulty is that an investigation of the inelastic pion production by negative pions of $\sim$1 Bev energy incident on hydrogen, Walker *et al.* (31) conclude that the experimental evidence does not support this model.

One recent approach (32) has been to associate the rise in the $T=\frac{1}{2}$ cross-section with the formation of the already known nucleon isobar with $T=J=3/2$ followed by its subsequent decay via pion emission. This approach appears promising in explaining the general behavior of the total cross-sections and also the characteristics (32, 33) of the inelastic pions.

The treatment of the production of pions by pions incident on nucleons via the Chew-Low formalism (34) has also been considered recently.

Causality and dispersion relations.—The Kramers-Kronig dispersion relation for light was derived from the condition that the scattered wave amplitude should be zero until the incident wave reached the scatterer. and that signals cannot propagate faster than the velocity of light. Such causality relations which relate the real part of the forward scattering amplitude to an integral over the imaginary part have recently been developed for pion-nucleon scattering by Karplus & Rudeman (35) for the scattering of neutral pions, and later by Goldberger and co-workers (36) for charged pion scattering. Anderson *et al.* (22) have found that they can be used successfully in deducing the forward scattering amplitude for $\pi - p$ scattering via integrals over the total cross-sections.

Dispersion relations for scattering at all angles have recently been proposed by several groups (21, 37). In regard to the validity of these relationships one might note that until recently the best support for them was that for pseudoscalar couplings, these hold in all orders of perturbation theory.

Recently, Symanzik (37) has proved these relations for the forward direction and for infinitesimal angles under certain conditions. Bogoliubov (38) has proved them for any finite angle.

They have been applied to reject some of the many phase shift solutions of $\pi^+ - p$ scattering (22) and in fact in a recent application (21), appear to discriminate against the Yang set and support the Fermi set. The spin-flip amplitudes were used, which in effect is equivalent to performing a theoretical polarization experiment.

As pointed out by Goldberger and co-workers (36) with certain assumptions one can get equations similar to Low's integral equations for the phase shifts.

The dispersion relations depend only on microscopic causality, Lorentz invariance, and several general relations for local field theories. Therefore they represent a general equivalent for the usual concepts of conventional local field theory.

Coupling constant.—The renormalized, unrationalized coupling constant f^2 deduced from the Serber-Lee plot in Figure 2 is $f^2 = 0.107 \pm 0.01$. If a Chew-

Low plot (not shown) had been used one would have obtained $f^2 = 0.96 \pm 0.01$ or about a 10 per cent smaller number.[8] The experimental errors are at present larger than the difference in the two methods. A straight line extrapolation for a coupling constant determination from a nonspin-flip dispersion relation has been used by Haber-Schaim (39) who obtained $f^2 = 0.082 \pm 0.015$. This dispersion relation is rapidly convergent and probably represents the most accurate extrapolation that can be made at this time. Bernardini and co-workers (40a) have obtained from their experiments on photoproduction, a zero point determination of the coupling constant $f^2 = 0.067 \pm 0.003$. The Bernardini value is not inconsistent with the Haber-Schaim value based on dispersion theory within the errors. It has been pointed out by Puppi & Stanghellini (41a) that the significantly lower results of the Bernardini and Haber-Schaim coupling constant determinations from those previously obtained for the Serber-Lee or Chew-Low plots may be due to the fact that the Serber-Lee and Chew-Low plots consider scattering in the $T = J = 3/2$ state while both the photoproduction and dispersion theory [Haber-Schaim] determinations involve the $T = \frac{1}{2}$ state also. Puppi (41b) finds that the predicted coupling constant based on applying causality to $\pi^- + p$ scattering only is much smaller. A recent determination by Davidon & Goldberger (21b) of f^2 using spin flip-amplitudes from dispersion theory which depend on α_{33} and α_{31} has yielded $f^2 \approx 0.1$ for the Fermi set. Hence, it appears that determinations of f^2 which involve pure $T = 3/2$ states seem to yield higher values than those which involve $T = \frac{1}{2}$ states as well. Errors in the evaluation of the various extrapolation procedures, or electromagnetic effects (41c, 41d, 41e) do not appear to be large enough to account for the discrepancies. If the experimental results are correct, either charge independence or more likely microscopic causality appear to be violated. However, an underestimation of electromagnetic effects or an incorrect evaluation of the dispersion integrals at high energies may possibly be the explanation (41b, 41c, 41d, 41e).

Collisions of Positive and Negative Pions with Heavier Nuclei

Cross-sections.—The total cross-sections of deuterium for negative pions has been recently measured with counter techniques from 128 to 400 Mev (2, 42) and 0.8 to 1.9 Bev (25). One can represent the deuterium cross-section by the sum of the individual pion-nucleon cross-sections plus a correction term as follows:

$$\sigma(\pi^- + D) = \sigma(\pi^- + n) + \sigma(\pi^- + p) + \Delta \qquad 7.$$

If it is then assumed by the principle of charge symmetry that $\sigma(\pi^- + n) = \sigma(\pi^+ + p)$, one finds from these experiments that Δ is negative and of the order of 15 per cent or less of $\sigma(\pi^- + D)$. Both its sign and magnitude can be

[8] A value of $f^2 \approx 0.010$ has also been obtained from Low's equations by Cini & Fubini (90).

reasonably explained by interference (43) and shadow (44) effects. This supports the principle of charge symmetry.

Some measurements have also been made for $\sigma(\pi^+ + D)$ at 120 to 180, 550 and 740 Mev (2, 25). In all cases it was found that within the errors $\sigma(\pi^+ + D) = \sigma(\pi^- + D)$ which strongly supports the principle of charge symmetry. Rogers & Lederman (45a) have investigated the scattering of 85 Mev positive pions in a deuterium filled diffusion chamber, and also find results consistent with the sum of the free nucleon scattering cross-section when interference effects (45b) are taken into account.

The total cross-sections of Be, C, and O and the inelastic collision cross-sections of Be, C, Cu, and Pb for 140 to 400 Mev π^- mesons have been measured with counter techniques by Ignatenko *et al.* (46). For the light nuclei both the total and the inelastic cross-sections follow the general energy behavior of the pion-hydrogen total cross-sections (see Fig. 3); however, the region near the peak cross-section relative to the tails is smaller and broader. The total and inelastic cross-sections are relatively constant in the energy interval of 140 to 250 Mev but drop fairly rapidly thereafter. For the heavier nuclei the energy variation of the cross-sections is smaller, as one would expect, which is attributable to the increasing importance of the shadowing of nucleons by others. The shadowing effects also qualitatively explain the previously noted behavior of the cross-sections of light nuclei.

In general, the behavior of the total and inelastic cross-sections of Be, C O, Cu, and Pb for negative pions in the energy range 140 to 400 Mev has been found by these authors to be consistent with the predictions of the optical model (47, 48) with a nuclear radius of $1.42A^{1/3} \times 10^{-13}$ cm. The observed results were not sensitive to the effects of the Pauli Exclusion Principle for incident pion energy $\gtrsim 150$ Mev.

Total cross-sections for Be, C, Al, Ca, and the inelastic cross-sections of Be, C, Al, Ca, Cu, Sn, and Pb for 970 Mev π^- have been determined by Abashian *et al.* (49). These authors find their results are consistent with the optical model when it is modified by using the shape of the nucleus deduced by Hofstadter and co-workers (50) and a radius about 5 per cent larger than the electromagnetic radius. Williams (51) has analyzed the elastic and inelastic cross-sections of emulsion nuclei for 1.5 Bev negative pions and finds an approximate agreement with the optical model for a tapered
51). Some general comments in regard to the different nuclear radii and density distributions used by various authors will be made in the last section of the paper in connection with an analysis of the optical model for nucleon-nucleon collisions.

Elastic and inelastic scattering.—Differential elastic scattering of 80 Mev positive and negative pions has been investigated by Pevsner *et al.* (52) for Al and by Williams *et al.* (53) for Li and Cu. The differential elastic scattering cross-sections of Cu and Al drop rapidly from values of $\sim$1,000 mb per steradian at $\theta \sim 15°$ to values of $10 \gtrsim$ mb per ster. at $\theta 7 \gtrsim 5°$. For Cu and Al the

experimental results were in reasonable agreement in the forward hemisphere with the predictions of an exact optical model phase shift calculation (52, 53) using a complex attractive square well potential for $r \leq 1.4A^{1/3} \times 10^{-13}$ cm. and the Coulomb potential for $r > 1.4A^{1/3} \times 10^{-13}$ cm. The calculations were performed by actually solving the Klein-Gordon equation for the angular momentum states which contribute appreciably, using a square well with suitable boundary conditions which include matching external Coulomb wave functions. The optical model predictions beyond the first diffraction minimum departed progressively with angle from the experimental results. In particular, the experimental results indicated too large a cross-section in the backward direction and did not show the well defined subsequent minima and maxima present in the theoretical diffraction pattern results.

These authors felt that at the larger angles inelastic transitions accepted within the experimental energy resolution, the width of the angular resolution and the possible effects of a tapered edge nucleus could probably account for the observed discrepancies. In a continuation of this work [see note added in proof, (53b); (54)] with a new detection method which greatly increased discrimination against inelastic events, reasonable indications of diffraction patterns were found, and a general behavior in agreement with the predictions of the optical model was observed. The remaining discrepancies with the theoretical predictions can probably be attributed to the effects previously mentioned above.

All experiments show a characteristic interference of the nuclear and Coulomb scattering which is destructive for π^+ and constructive for π^- implying a positive sign for the α_{33} phase shift. Several modified Born approximation calculations (52, 53) in which coherent additions of π-nucleon scattering from individual nucleons are multiplied by suitable form factors and attenuation factors were also performed, and the results agree reasonably well with the experimental behavior for the forward angles. The complex nuclear potential was included in the energy term in the Klein-Gordon equation as the fourth component of a four-vector. The potential which fits the results for Al and Cu reasonably well is approximately a uniform well with a real part $\sim$30 Mev deep and an absorptive imaginary part $\sim$20 Mev. One should note that the theoretical results are not very sensitive to small variations of these values.

In the case of pion-lithium (53) elastic scattering the Born approximation calculation was in reasonable agreement with the experimental data at all angles, and it appears to be a much more suitable treatment than the optical model for the case of very light nuclei at low pion energies. It is obvious that the usual optical model approximation of a uniform complex potential within a definite radius would improve for large nuclei and higher energy pions with a correspondingly smaller deBroglie wave length.

The elastic and inelastic scattering of pions in the energy range 230 to 330 Mev have been investigated recently by Dzhelepov *et al.* (55) in carbon

and Pb plates in a Wilson chamber; by Kozodaev and his associates (56) in a helium diffusion chamber, and by Mitin & Grigoriev (57) in photographic plates. These experiments have also been treated in a review by Ignatenko (58). The predictions for the elastic scattering of pions in carbon and helium have been computed for the optical model and are consistent with the experimental results. These results are only significant for scattering angles less than 50° due to the limited statistics, and the fact that the elastic scattering cross-section drops rapidly with increasing angle.

One of the most significant features of the inelastic pion scattering is the large loss of pion energy which is ~150–220 Mev on the average. This is interpreted (58) as evidence for several collisions of the incident pion with individual nucleons in the nucleus. This would be expected especially for emulsion and Pb nuclei considering the short mean free path in nuclear matter of pions in this energy range. Further support for this hypothesis of several individual pion-nucleon collisions is the observed changes in the angular distribution of inelastically scattered pions both with angle and also increasing atomic weight. The angular distribution in carbon is similar to that expected for the scattering of negative pions on free nucleons. The results in emulsion and Pb are quite different, however, in the backward direction similarity to the scattering by free nucleons is greatest, and conversely in the forward direction the changes are greatest. This can be explained by the fact that the pion mean free path in nuclear matter is very small at these energies so that the first interactions would take place near the surface. Hence a backward scattered pion has more chance of escaping without a second scattering, whereas those emerging in the forward direction would have in general had to interact several times. The observed relations of the energy loss of pions to the scattering angle have been compared to the calculated relations for single collisions. This comparison implies that multiple collisions are common for the forward angles and become less important for the backward ones, which is consistent with the previous conclusions.

The interaction of 750 Mev π^--mesons with emulsion nuclei have been investigated by Blau & Oliver (59a). They find that inelastic meson scattering with the production of a second meson by the incident one is an important process which is estimated from the observed cases to occur ~40 per cent of the time at 750 Mev and was previously estimated to occur ~10 per cent of the time at 500 Mev (59b). The mean prong number of the stars without escaping mesons is ~four at both energies and $\lesssim$three for stars containing an outgoing meson. These observations are also consistent with several collisions of the incident meson with final absorption of it by the nucleus accounting for ~40 per cent of the cases at 750 Mev. The stars in general do not exhibit the characteristic forward nucleon cascade of grey tracks seen in nucleon induced stars produced by fast nucleons.

Approximately 7 per cent of the stars (at 750 Mev) of more than five prongs exhibited fragments ($Z \geq 3$) compared to a frequency of less than 1 per cent for stars induced by nucleons of 200 to 400 Mev for which meson

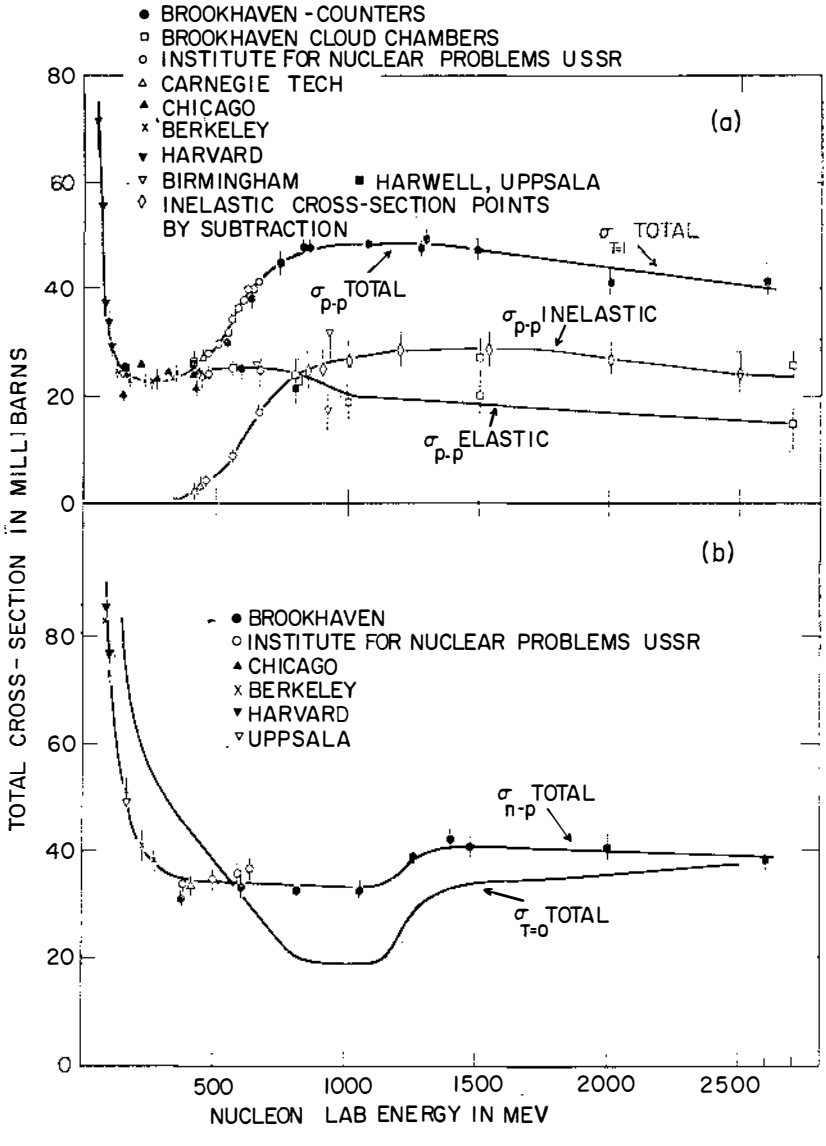

FIG. 4a. The p-p total, the elastic, and the inelastic cross-section as a function of energy. All curves shown are empirical. The open diamond points have been obtained by a subtraction of the elastic cross-section curve from the total cross-section curve and estimated errors are attached. In the region beyond 300 to 400 Mev, the errors on elastic points have been made by broken lines so that they may be distinguished from inelastic or total cross-sections. Since p-p contains only the $T=1$ state the cross-sections are equal to the corresponding ones for the $T=1$ state (61 to 65).

FIG. 4b. The total n-p cross-section is shown as a function of energy. The $T=0$ total cross-section deduced from the total p-p and total n-p (see text) is also shown. All curves are empirical (61, 67, 68).

production is infrequent. Furthermore, mesonless stars were relatively rich in fragments implying strongly that meson absorption is responsible for fragment emission.

Collisions of Nucleons with Hydrogen and Deuterium

p-p collisions.—The behavior of the *p-p* cross-section as a function of energy has previously been fairly thoroughly investigated from low energies to about 400 Mev by various groups using the several F. M. cyclotrons available in this energy range for some time.

The total *p-p* cross-section [see Fig. 4a] is approximately constant from 150 to 350 Mev, and the angular distribution is more or less isotropic outside the region of coulomb interference

The theoretical explanation of these characteristics is not completely clear, however, considerable progress (60) has been made recently in fitting both *p-p* cross-sections and polarization experiments.

Recently, the new higher energy machines at Brookhaven, 3 Bev, (61, 62); U.S.S.R. Institute for Nuclear Problems, 660 Mev (63); and Birmingham, 1.0 Bev (64) have been used by several groups to extend the measurements of total, elastic, and inelastic cross-sections to beyond 2.0 Bev.

Figure 4a shows the latest compilation of *p-p* cross-sections including these higher energy points (61 to 64) and also some lower energy work[9] (65). The most extensive investigations have been made by Meshcheriakov, Dzhelepov, and co-workers (63), Chen *et al.* (61), Shutt and co-workers (62), Smith *et al.* (61a), Batson *et al.* (64a) and Hughes *et al.* (64b). The total and elastic cross-section measurements have been mostly made directly, however, inelastic cross-sections have been determined both directly and also by subtraction of the elastic from the total cross-sections.

The most striking feature in the new results is the rapid increase of the inelastic cross-section from near zero at 350 Mev to about 25 mb at 800 Mev and its more or less constant value (25 to 30 mb) at higher energies. The elastic cross-section on the other hand remains fairly constant ($\sim$25 mb) from 350 to 800 Mev and decreases slowly thereafter to about 15 mb at 2.6 Bev. Due to the relative constancy in the elastic cross-section the total cross-section, which is the sum of elastic and inelastic, essentially shows the same sharp rise of about 25 mb as the inelastic cross-section does between 350 and 800 Mev followed by a more or less constant cross-section thereafter. The rise in the inelastic cross-section from 350 to 800 Mev has been found experimentally (62, 64) to be composed almost entirely of single pion production below 1.0 Bev incident proton energy.

The differential elastic scattering cross-section above 400 Mev (61, 62, 63) has shown a rapid change from the former ($\lesssim$350 Mev) isotropy to an

[9] See the table on pp. 222 to 223 of Chen *et al.* (61) for a recent summary used which includes references to the older low energy work.

increasingly forward peaked distribution which at $\gtrsim$0.7–1.0 Bev is in general characteristic of the expected diffraction pattern (61 to 64, 66) accompanying the inelastic absorption of the incident wave.

n-p and p-d collisions.—The behavior of the *n-p*, total cross-section as a function of energy, is shown in Figure 4b. Although a few points (67, 68) beyond 400 Mev have been obtained directly, most of the higher energy data (61) has been determined by the difference between *p-d* and *p-p* to which is added a correction (positive throughout) for interference effects which correspond to $\lesssim$20 per cent of the *n-p* cross-section. The error on this correction is probably a small fraction of it, due to the fact that the observed differences between several points of *n-p* measured directly and the indirect method described are small.

Assuming charge independence, a separation of the *p-p* and *n-p* total cross-sections has been made into the two isotopic spin states involved, ($T=0$ and $T=1$) according to the well known relations:

$$\sigma_{T=1} = \sigma_{p\text{-}p} \qquad 8.$$

$$\sigma_{T=0} = 2\sigma_{n\text{-}p} - \sigma_{p\text{-}p} \qquad 9.$$

The results are shown in Figures 4a and 4b. The total $T=0$ cross-section ($\sigma_{T=0}$) continues to follow its lower energy behavior and continuously decreases in the region of 400 to 800 Mev, and then levels off at a minimum value to beyond 1 Bev, after which it increases rapidly from ~1.1 Bev to ~1.5 Bev and only slowly thereafter. Hence it appears that in the region of 400 to 800 Mev while single pion production is rapidly increasing in the $T=1$ state, which is accompanied by the sudden rise in $\sigma_{T=1}$, this does not appear to occur in the $T=0$ state. Dzhelepov *et al.* (67) have deduced a value for the inelastic cross-section in the $T=0$ state of 9 ± 4 mb at 580 Mev by subtraction methods. The large errors and uncertainty in the cross-sections used in the subtraction method make it difficult to decide that the real value is different from zero within all possible errors.[10] On the other hand, double pion production is known (62, 69) to set in rapidly in the $T=1$ state between 1.0 and 1.5 Bev while in this energy range the $T=0$ state shows a sharp rise of ~17 mb similar to that shown by the $T=1$ state in the region of 400 to 800 Mev. This is observed experimentally (70) to be accompanied by a much larger ratio of double to single pion production in *n-p* collisions than in *p-p*. Hence, it is implied that only double pion production can occur in the $T=0$ state while both single and double pion production can occur in the $T=1$ state. This is additional support for the assumption to be discussed later that pion production proceeds through excitation of a nucleon to the resonant $T=J=3/2$ (isobaric) state observed in the pion-nucleon scattering. For this case, zero, one or two, $T=J=3/2$ nucleon isobars for elastic scatter-

[10] A. P. Batson, B. Culwick, and L. Riddiford have recently determined that the inelastic cross-section in the $T=0$ state is zero within the errors at 950 Mev (91).

ing, single, or double pion production respectively can be formed in a $T=1$ state. However, either zero or two $T=J=3/2$ nucleon isobars for elastic scattering or double pion production respectively can be formed in a $T=0$ state.

The fact that in the $T=1$ state neither the total nor the inelastic cross-section increases much further when double production sets in can be explained by assuming that a saturation of the inelastic cross-section has already occurred with single pion production and this cross-section $\sim$27 mb corresponds to the size of the region in which inelastic interactions occur.

One should remark here that neither charge symmetry or charge independence have been found to be violated by any of the experiments performed to date.

Pion Production

In p-p and n-p nucleon-nucleon collisions producing a single pion all of the reactions consistent with charge conservation have been previously observed (1, 71), and are listed below:

(*a*)	$p+p$	$p+n+\pi^+$	(*e*)	$p+n$	$p+p+\pi^-$
(*b*)	$p+p$	$p+p+\pi^0$	(*f*)	$p+n$	$p+n+\pi^0$
(*c*)	$p+p$	$D+\pi^+$	(*g*)	$p+n$	$D+\pi^0$
(*d*)	$p+n$	$2n+\pi^+$			

The corresponding n-n reactions are related to (*a*), (*b*), and (*c*) by the principle of charge symmetry.

Reactions (*c*) and (*g*) dominate pion production near threshold ($\sim$300 to 400 Mev). However, as the energy increases, the cross-section for (*c*) increases rapidly to a peak reported value (72) of 3.1 ± 0.2 mb at 660 Mev and drops rapidly thereafter to a value of $\sim$0.5 mb beyond 800 Mev (62, 64). Reaction (*g*) is not as well determined experimentally but the general behavior is probably the same. These two reactions have been adequately explained (71, 73) as a consequence of the large final state interaction of the two slow nucleons in the deuteron state when mesons are produced near threshold. Hence they rapidly become less important with increasing energy. The same is obviously true for the inverse reaction to (*c*) which is pion absorption in deuterium leading to a two nucleon final state. Several well known phenomenological treatments of pion production which make use of charge independence, a consideration of the properties of the nucleon-nucleon final states including interactions, and various assumptions about matrix elements for meson production have been described elsewhere (1, 71, 73) and will not be considered here. One might generally remark that these methods are most suitable near the pion threshold where they were originally applied, and their usefulness decreases rapidly with increasing energy.

Many investigations of reactions (*a*) and (*b*) and the corresponding unbound reactions for double pion production have been performed recently

in the energy range beyond 400 Mev. Pion production in p-p collisions has been observed with hydrogen filled chambers (62, 64, 74) at 380, 650, 800 Mev, 1.5 and 2.75 Bev, with counters (69, 72) from 440 to 660 Mev, 1.0 and 2.3 Bev, and with emulsions (64, 72) at 660 and 925 Mev.

The total pion production cross-section is given as a function of energy by the inelastic p-p cross-section curve in Fig. 4a. The rapid increase below 1.0 Bev is due to single pion production since double production is small below 1.0 Bev. Beyond 1 Bev double pion production increases rapidly until $\sim$2 Bev with only small increases thereafter (62, 69). The ratio of cases of double production to single production changes from $\lesssim$1:20 at 0.8$-$1.0 Bev to $\sim$1:3 at 1.5 Bev to $\sim$1–1.5:1 in the range 2.0 to 2.7 Bev[11] (62, 69).

A remarkable general similarity of the energy spectra of the pions[12] (see Fig. 5) in the nucleon-nucleon c.m.s. is exhibited by all of the experiments in the energy range of 0.8 to 2.3 Bev (62, 64, 69). All c.m.s. pion energy spectra show a peak at $\sim$100 to 200 Mev and a general similarity to the $\pi^+ + p$ total cross-section (see Fig. 3) in the energy range (0 to 500 Mev). The peak in the $\pi^+ + p$ total cross-section at $\sim$180 Mev in the lab system corresponds to a peak at $\sim$120 Mev in the c.m.s. Of course the high energy cut-off and the width of the peak in the pion energy spectra both increase with energy. At the higher energies $\sim$2.0 Bev the single pion energy spectrum is broader than the double pion energy spectrum which is closer in appearance to the $\pi^+ + p$ total cross-section curve. This general similarity in the pion energy spectra extends down to 660 Mev if one does not include the effects of the deuteron formation which adds a high energy peak to the spectrum. The similarity at 660 Mev (72) is particularly noticeable at wide angles (46°) in the lab system since the deuterons and their associated π^+ are peaked near the beam direction. This angle (46° lab) corresponds for the pions to $\sim$77 $-$90° in the c.m.s.

The energy spectra predicted by the Fermi statistical theory (92) for each multiplicity are completely determined and independent of the volume. Comparisons of the Fermi spectra for the individual multiplicities and also appropriately combined with the observed experimental multiplicities to obtain predictions for the total pion spectrum have been made (62, 64, 69, 75). Except in special cases, where the agreement appears accidental (75), the Fermi theory disagrees badly with experiment mainly because there are too many high energy pions and too few low energy pions.

[11] Triple pion production is observed at 2.7 Bev to occur in $\sim$15 per cent of all inelastic interactions.

[12] Most of the detailed investigations have been made for π^+ which accounts for $\sim$80 per cent of the single pion cross-section and is easy to measure experimentally. The energy spectra of π^0 are obviously more difficult to obtain, but where checked (72) exhibit this general similarity. The production of π^- in p-p collisions only occurs in double production and to date only fragmentary information exists which is generally consistent with the foregoing.

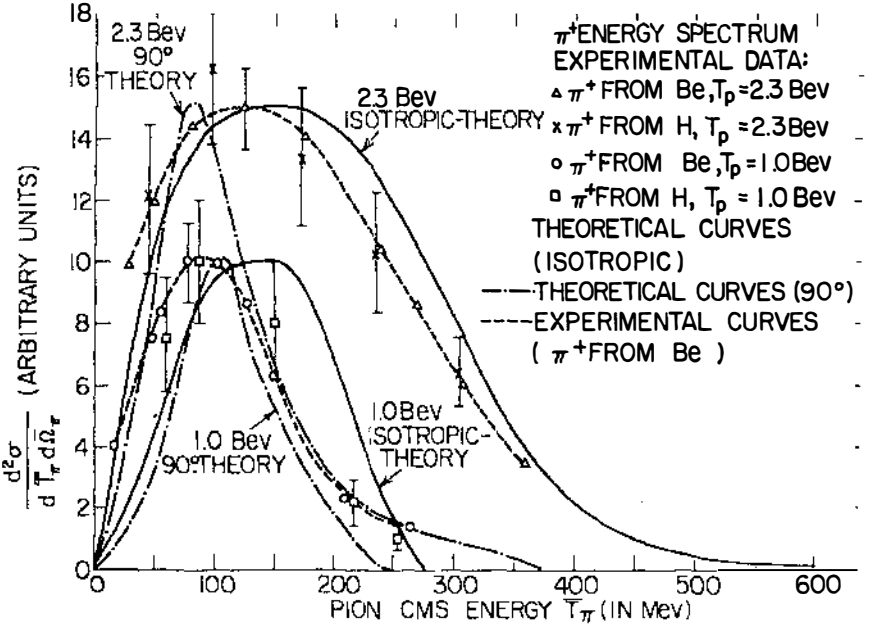

FIG. 5. The π^+ energy spectra from p-p and p-Be collisions at $T_p = 1.0$ and 2.3 Bev (69) are given and compared to calculations (75) based on an isobaric nucleon model (discussed in text). Results for isotropic, and only forward and backward, emission of isobars in the c.m.s. observed at ~90° [labelled 90° theory] are shown. The experimental data corresponds to pion emission angles in the c.m.s. of ~60 to 75° at 1.0 Bev and ~73° to 105° at 2.3 Bev. An analysis of the cloud-chamber experiments (62) indicates isotropic pion emission at 2.3 Bev and a considerable amount of forward-backward peaking at 1.0 Bev which therefore implies reasonably good agreement of the calculations with the data. The cloud chamber data (not shown), although of considerably lower statistical accuracy and momentum resolution, are in general agreement with the counter data.

The general qualitative features of the experimental pion energy or momentum spectra have been explained by the hypothesis that both single and double pion production proceeds through excitation of one or both nucleons respectively to the isobaric state of $T = J = 3/2$ (69, 70, 75) previously observed in the $\pi^+ + p$ scattering resonance at ~190 Mev. Quantitative agreement with the experimental π-meson energy spectra in p-p collisions has been obtained at energies of 0.8 Bev, 1.0 Bev, 1.5 Bev, and 2.3 Bev with an isobaric nucleon model by Lindenbaum & Sternheimer (75). [See Fig. 5 for 1.0 and 2.3 Bev π^+ spectra.] The relative probability for isobar formation and subsequent decay with a variable total energy in the isobar rest system was phenomenologically related to the total $\pi^+ + p$ scattering cross-section.

Another difficulty with the Fermi theory is the inability to explain the

sudden increase of double pion production beyond 1 Bev with a volume corresponding to the Compton wave length of a pion (62, 69, 75). The experimental inelastic cross-section actually corresponds to a black sphere much smaller than this, which would make the disagreement even more marked. On the other hand, the isobaric nucleon model (75) predicts the correct general behavior for the double pion production. The observed branching ratios of various charge states (62, 75, 76), Q value distributions between pions and nucleons, and the angular correlation between pions and nucleons (62) are also in reasonable agreement with the predictions.

Investigations of n-p pion production in hydrogen filled chambers (70) for effective incident energies of $\sim$1.1 and 1.7 Bev have revealed many of the general features of pion production found in p-p collisions. However one notable exception is the considerable increase in double relative to single production. This is also in qualitative agreement with the predictions of the isobaric nucleon model since as previously pointed out, only double pion production can occur in a $T=0$ state since one $T=3/2$ isobar cannot be combined with a $T=\frac{1}{2}$ recoil nucleon to form a $T=0$ state. A quantitative agreement has also been obtained (75). The energy spectra of π^+ and π^0 mesons and the π^+/π^0 ratio for mesons produced in p-p collisions at 556 and 667 Mev also appears to be consistent with the formation of a nucleon isobar (72).

A modification of the Fermi statistical theory by Kovacs (77) to include relative enhancement of those final states for which the pion nucleon interaction is large, has yielded reasonable predictions for the branching ratios of various charge states and the behavior of the pion multiplicity as a function of energy (62, 70)

Lepore & Neumann (93) have developed a relativistic phase space theory which conserves the relativistic center of energy and thus reduces the volume of phase space accessible to high energy pions. This effect tends to modify the energy spectra in the right direction but, of course, will not provide the many clear-cut characteristics of the $T=J=3/2$ state that seems to pervade the data at these energies.

Belanki & Nikishov (78) have found that inclusion of isobars in the statistical theory yields reasonable agreement for various charge state ratios and the behavior of the multiplicity with energy.

One should note that the experiments on pion production in nucleon-nucleon collisions have established the dominant features of the interactions; however, the details are not definitely determined. For example, 50 to 100 events are involved in many of the experimental pion spectra obtained by cloud chambers. The counter experiments on the other hand provide more accurate energy spectra but are less complete in that all the details of an individual event are not measured together. One should keep the foregoing in mind relative to the experimental agreements with theories, which while encouraging in general features do not necessarily imply agreement in the finer details.

Charged pion production in beryllium has been studied with counter

techniques at 660 Mev (72), 1.0 Bev and 2.3 Bev (69) and at 2.2 Bev with emulsions (79). Carbon has been studied at 660 Mev (72). The observed pion spectra and other general properties of these reactions are very similar to those observed in p-p (see Fig. 5) and n-p collisions. This is true at 660 Mev only if the unbound reaction (without deuteron formation) is considered.

As a matter of fact, originally the p-Be pion spectra (69) at 1.0 and 2.3 Bev were successfully analyzed on the assumption that essentially free nucleon-nucleon collisions occur without important changes in properties due to subsequent interaction.

One should note here that the energy spectra of π^+ produced in Be at wide angles in the c.m. system are generally similar at 660 Mev, 1.0 and 2.3 Bev. The π^- energy spectra also have the same general properties

The average mean free path for pions near the resonance energy is $\sim 10^{-13}$ cm., however, on both sides of this peak it increases very rapidly so that the average mean free path is probably $2\text{–}3\times 10^{-13}$ cm. for the observed pion spectra in the incident nucleon energy range of 0.6 to 3.0 Bev.

In even the lightest nuclei this average mean free path is of the order of a radius ($\sim 3\times 10^{-13}$ cm. for Be). However, since many of the nucleons are near the surface a fair share of the pions can escape with zero or perhaps one collision following production.

In the heavier nuclei $A \sim 100\text{–}200$ the radius is $\sim 6\text{–}9\times 10^{-13}$ cm. and hence many free paths. As previously noted, single pion production increases rapidly beyond 400 Mev to the order of half the total p-p cross-section ($T=1$) above 800 Mev and double pion production becomes large in both the $T=1$ and the $T=0$ states above $\sim 1.2\text{–}1.5$ Bev.

The combination of a large mean pion production per nuclear interaction (estimated to be ~ 0.8 at 1.0 Bev and ~ 1.5 at 2.0 Bev) coupled with the short mean free path of the low energy pions produced in heavy nuclei, obviously implies a series of additional scatterings of these pions. In many cases their eventual absorption either directly or after slowing down to <150 Mev where the two-nucleon absorption becomes large is also to be expected. Hence a mechanism for increasingly large transfers of excitation energy to a nucleus is present as the incident nucleon energy increases above the pion production threshold. This is in contrast to the more or less constant low average values of the excitation energy (~ 50 Mev) transferred to the nucleus by the nucleonic cascades resulting from elastic collisions below 400 Mev (80). This general mechanism for large excitation energy transfers to nuclei has been previously postulated by Friedlander and co-workers (81) and then by Lock *et al.* (82) to explain their experiments.

The hypothesis of the interaction of incident nucleons of 100 to 400 Mev with nucleons of heavy nuclei, as if they were free except for the Pauli Exclusion Principle effects, has been successful in explaining the experimental results for Ag-Br nuclei in emulsions (80). The struck nucleons together with

the incident ones are considered to interact in the same manner until they either reach the edge of the nucleus with an energy greater than the effective potential and escape or else lose sufficient energy to drop below the nuclear potential barrier and be captured.

The thermal excitation transferred to the nucleus in this model is due to both captured nucleons and the excitation due to holes left in the energy momentum distribution. Subsequent boiling off or evaporation of nucleons and some heavier particles is the end result. This thermal excitation is reasonably constant and is of the order of 50 Mev for incident nucleon energies from 90 to 400 Mev (80). Considering elastic nucleon-nucleon scattering collisions only the estimated average contribution to thermal excitation by a 1 Bev nucleon is ~70 Mev (80, 82). If on the other hand at 1.0 Bev approximately $\frac{1}{3}$ of the time one pion of mean total energy ~300 Mev is produced and absorbed in a heavy nucleus, an additional excitation energy ~100 Mev average is contributed to give a total average excitation of ~150 Mev. At 2.0 to 3.0 Bev, due to the increase in double and plural production, one might expect perhaps twice this additional excitation corresponding to a total average excitation energy of perhaps 250 Mev. Obviously the statistical fluctuations will allow a wide distribution of thermal energies with a large fraction of the incident energy transferred to thermal excitation in some cases. This thermal excitation may never approach the simple concept of a uniform equilibrium temperature but may rather be characterized by a random distribution of local hot spots with local disintegration before equilibrium is established.

Characteristics of the Inelastic Interactions of Nucleons with Nuclei

The nuclear interactions of 600 Mev and 950 Mev protons with the nuclei of G-5 emulsion have been studied by Lock *et al.* (82, 83a). In general they find that π-meson production greatly affects the characteristics of the interactions at 950 Mev and has some effect even at 600 Mev.

The prong distribution of stars at 600 Mev is similar to that at 400 Mev except for a slight increase in large prong numbers. At 950 Mev there is a great increase in stars with ≥ 6 prongs (by a factor of 3) and a corresponding decrease in the smaller stars . This behavior has been qualitatively explained by the large increase in single pion production at 950 Mev.

Some crude estimates of the development of the nucleonic cascade in the heavy emulsion nuclei (Ag-Br) including meson production and reabsorption were made by these authors and compared to stars in Ag-Br. They find that the mean prong number of grey plus shower tracks (protons >30 Mev) and black tracks (protons <30 Mev) can be approximately explained. An average thermal excitation of 70 Mev was taken for 40 per cent of the cases in which meson production is assumed not to occur and 25 per cent of the cases for which meson production does occur but the meson escapes. In approxi-

mately 35 per cent of the cases it was assumed that a meson was created and reabsorbed resulting in an average thermal excitation of 210 Mev. This procedure gives a mean thermal excitation of ~120 Mev for all interactions.

The black protons seem to be more isotropic than at lower energies and follow an evaporation spectrum calculated for the estimated mean thermal excitation. The process of meson production and absorption seems to have washed out some of the forward peaked behavior and lowered the mean energy of the black knock-on protons observed at lower energies (80). However, there is still reason to believe from the cascade calculations that ~20 per cent of black protons are still of knock-on origin.

There is some evidence that α-particles are forward-peaked in angle and it is concluded that some are also ejected in the cascade from heavy nuclei at 950 Mev. This latter process may well be connected with meson absorption as it was previously noted, that in pion induced stars fragment emission is enhanced.

McKeaque (83b) (cf. also ref 82b), has separated the disintegrations predominantly induced in light nuclei of the G-5 emulsion by 950 Mev protons. A discussion of the method is presented in the papers. The general characteristics of the stars in light and heavy nuclei are remarkably similar in regard to mean prong numbers of total, shower, grey, and black prongs. However, the prong distribution in light nuclei is peaked at about five and is small or zero above 8 prongs, while in heavy nuclei the prong distribution is peaked at about one or two and extends to ~15 prongs. The black protons and α-particle spectra both have a peak at ~4 Mev for light nuclei corresponding to peaks at ~7 and ~11 Mev respectively for heavy nuclei.

These characteristics are consistent with the interpretation that in light nuclei smaller cascades are developed followed by a thermal evaporation or break-up of the nucleus into several very low energy protons, alphas, and other fragments. In the heavier nuclei, on the other hand, more extensive cascades are developed with a more complete sharing of the incident proton energy among a greater number of particles, and a resultant larger thermal excitation. Therefore the sharper distinction in energy found in light nuclei between the knock-ons and the particles due to evaporation or break-up of the residual nucleus is reduced in the case of heavy nuclei. The differences in prong distribution also reflect the effect of a more extensive cascade in the heavier nuclei.

Some evidence is also present in this analysis for the possible interaction of the incident proton with sub groups (mainly α) of the light nucleus, in this and other experiments, quoted in (83), at lower energies.

Another approach to the study of inelastic interactions of high energy protons with nuclei is the radio chemical method for determining the distribution of residual nuclei resulting from bombardment of a heavy nucleus. The products resulting from bombardment of bismuth with protons of 340 Mev [Biller (84a)], 480 Mev [Vinogradov *et al.* (84b)] and 660 Mev [Murin

et al. (84c)] fall into two distinct mass regions: the so-called spallation region and the fission region. The spallation region refers to products with a mass number generally smaller than that of the target by less than 40 mass units and has a rapidly decreasing cross-section with decreasing A. The fission region has a peak at $A \sim 90$ to 95 and is characterized by a region of very low yield above $A \sim 140$ situated between the fission and spallation regions. The ratio of bismuth fission to total inelastic cross-sections increases monotomically from 0.06 at 100 Mev to 0.13 at 340 Mev and more slowly thereafter to 450 Mev (84).

Friedlander and his co-workers (81) found that for 2.2 Bev protons incident on bismuth and Pb, the valley between fission and spallation observed at lower energies disappeared. The formation cross-section for nuclides in the mass range $\sim$130 to 180 had increased by a factor of 4 from 480 Mev to 660 Mev (81, 84), but increased by two orders of magnitude when the proton energy was raised to 2 Bev.

A detailed study of the energy dependence of formation cross-sections of about 30 nuclides of $A \lesssim 140$ formed by the ineraction of lead with protons in the energy range 0.6 to 3.0 Bev has been reported, and thoroughly analyzed by Friedlander *et al.* (81). They find that the average energy transfer to the nucleus appears to change from the order 50 to 100 Mev at 400 Mev bombardment to $\sim$several hundred Mev for 3.0 Bev incident protons with an appreciable probability for energy transfers $\gtrsim$1 Bev. Their data clearly support their hypothesis that meson production is the vehicle for the greatly increased energy transfer above 400 Mev. Although the pion production cross-section increases only slowly beyond 1 Bev where single pion production seems to saturate, increases in the energy transfer seem to occur until 3.0 Bev. This is probably due to the increasing multiplicity of pion production and even the effects of plural production may be significant at 3.0 Bev. The increased probability of large energy transfers actually is expected to lead to a broad distribution of energy transfers from quite small to large values due to the large statistical fluctuations in the cascade mechanism.

At 3.0 Bev bombarding energy, spallation events involving 60 or 70 nucleons or their equivalent are found to be quite prevalent. The fission cross-section seems to decrease by a factor of $\sim$3 from 700 Mev to 3.0 Bev due to increasingly important competition from spallation and fragmentation.

The latter process was postulated (81) to account for product yields of $10 < A < 40$, and is pictured as a local rapid break-up or as a fast fragmentation of a small area of the nucleus, which has been highly heated locally by pion absorption or other effects. This is of course a different process than spallation which is thought to involve a thermal evaporation from the nucleus as a whole.

Actually it is questionable whether true spallation ever occurs at these high energies. One can seriously question the concept of an equilibrium

temperature in a greatly disrupted nucleus from which many nucleons have been ejected as knock-ons and which has absorbed an excitation comparable in many cases with its binding energy. Perhaps a more logical concept is that fragmentation occurs almost everywhere in the nucleus, but that in those areas where by chance or a sufficient thermal exchange with neighboring nucleons, or other local emission processes, the local temperature does not differ too much from the average temperature, the evaporated products can be considered as equivalent in properties to those which would correspond to a uniform average nuclear temperature. On the other hand, wherever there are large fluctuations in nuclear temperature, it is more fruitful to treat the particles emitted as originating from local hot or cold spots and so call them products of fragmentation. The connection between fragment emission and pion absorption has been previously observed in both pion induced stars and proton induced stars with associated meson production and absorption.

An extensive series of nuclear cascade calculations have been recently carried out at the Maniac Electronic Computer (85).

Previous Monte Carlo calculations (80) have been extended into the Bev region as well as improved statistically at lower energies. A three dimensional geometry was used and a cascade of nucleon-nucleon collisions including pion production and reabsorption were considered. The number, kind, energy, and the direction of the emitted particles in each cascade and the nature and state of the excitations of the residual nucleus were tabulated.

Incident energies ranging from 46 to 1,830 Mev for nucleons, and 0 to 1,500 Mev for pions were considered for various target nuclei which include Al, Cu, Ru, Ca, Bi, and U. About 1,000 cascades were computed for each interaction.

Some preliminary comparisons of the theoretical results with radio chemical and other data have been made and seem to yield a general agreement. The final compilation of these results and a systematic comparison with experimental data now available and also future data of sufficient accuracy for a detailed comparison should provide a critical test of the nucleonic cascade mechanism. One of the features which could still be considerably improved in this computation is the energy spectra assumed for the pion, which was based on an equal momentum for all particles in the c.m.s.

Total, Elastic, and Inelastic Cross-Sections of Nuclei for Nucleons

The inelastic and total cross-sections of various nuclei ranging from Be to Pb for protons and neutrons of various energies in the range 50 Mev to 1.4 Bev have been determined and analyzed (86, 87, 88, 51, 68). The basic optical model proposed by Fernbach, Serber & Taylor (47b) seems to still give a reasonable fit to the general features of the experimental data.

The simplest approximation to the optical model solution which was

originally used (47) is the assumption of a spherical complex well with a complex potential inside a radius R and no nuclear potential outside except the Coulomb field. The imaginary (absorptive) part of the potential is determined by the free nucleon-nucleon interaction cross-sections suitably modified by the Pauli Exclusion Principle and also the density of nuclear matter which in turn depends upon the radius assumed. The real part of the potential is generally adjusted to fit the data.

The results are usually expressed in terms of the three parameters, K the absorption coefficient in nuclear matter, k_1 the change in wave number upon entering the nucleus, and R the radius of the well. Refraction and reflection were neglected in the original simple treatment which was solved in analogy to the optical case for a uniform nuclear density. The inelastic cross-section depends only on K and R, and is experimentally the easiest to measure.

This simple picture seems to work at any one energy for the heavier elements but generally tends to require a radius $R=r_0A^{1/3}$ which involves higher values of r_0 for the light nuclei, but reasonably constant values for r_0 seem to suffice for the medium weight and heavy nuclei. The form $R=(b+aA^{1/3})$ fits the data for various nuclei better at any one energy but different values of a and b are required at various energies (87).

Furthermore the lower energy results ($<$100 to 200 Mev) seem to require for a spherical well radius $R\sim1.4$–$1.5A^{1/3}\times10^{-13}$ cm. for medium weight and heavy nuclei while the higher energy data (300 Mev to 1.4 Bev) seem to require $R\sim1.2$–$1.3A^{1/3}\times10^{-13}$ cm.

Several authors (51, 87) have attempted to improve the approximations involved in the optical model. A tapered nuclear edge which in effect is similar to the Hofstadter nucleon density distribution, reflection, and refraction at the nuclear surface, exact phase shift calculations, and other techniques have been used to attempt to obtain agreement with a nuclear radius which varies like $A^{1/3}$ in a consistent manner and is not too dependent on the incident energy. These procedures, notably the tapered edge, improve the situation considerably but it is not yet clear that all discrepancies can be removed. However, one might note that the sensitivity to the tails of the nuclear distribution obviously depends upon the cross-section of the incident particles for nucleons in the nucleus. A high cross-section increases the effects of the outermost regions of the nuclear distribution. Furthermore, there is an effective range of potential due to the finite size of the interaction range of the incident particle. Therefore it is not at all surpising that for incident particles with a high cross-section (lower energy nucleons) a relatively larger radius is required, and that these effects are magnified for the lighter nuclei. Similar effects have been previously observed in pion-nucleus interactions, where larger radii are required in the energy region where the pion-nucleon cross-sections are large.

The differential elastic scattering cross-section predicted by the optical model also seems to be in reasonable agreement where checked for smaller

angles than the first minimum (88). At and beyond the first minimum the details of the predicted diffraction pattern are quite sensitive to the nuclear density shape, the experimental angular, and elastic energy resolution, and also the dependence of the real potential on spin orbit coupling. However, for medium weight and heavy nuclei diffraction patterns in reasonable agreement with predictions have been observed (88). For the lightest nuclei, agreement is poor but the basic validity of the optical model approximation is more questionable and in fact difficulties in fitting the inelastic cross-section in light nuclei have been previously mentioned.

In the lightest nuclei the coherent elastic scattering cannot be expected to fit the optical model approximation, and indeed should to a certain extent exhibit the characteristics of the Born approximation estimate of the scattering from individual nucleons suitably modified by attenuation and form factors, as previously noted for elastic scattering of pions from light nuclei.

The analyses do not in general accurately determine k_1; however, it appears that k_1 probably is different from zero even near 1 Bev and corresponds to a real potential depth of $\sim$10 to 50 Mev where the latter value is the upper limit at 870 Mev (88).

There have been some indications from comparisons of neutron and proton results at low energies (87) that the distribution of neutrons in the nucleus has an effectively larger radius than the proton distribution. This interpretation is open to question at present and does not seem to be consistent with recent inelastic cross-section measurements of Pb for charged pions (49).

LITERATURE CITED

1. Gell-Mann, M., and Watson, K. M., *Ann. Rev. Nuclear Sci.*, **4,** 219 (1954)
2. Ashkin, J., Blaser, J. P., Feiner, F., Gorman, J. G., and Stern, M. O., *Phys. Rev.* **96,** 1104 (1954)
3. Lindenbaum, S. J., and Yuan, L. C. L., *Phys. Rev.*, **100,** 306 (1955)
4. Lindenbaum, S. J., and Yuan, L. C. L. (Private communication)
5. Ignatenko, A. E., Mukhin, A. I., Ozerov, E. B., and Pontekorvo, B. M., *Zhur. Eksp. i Teoret. Fiz.*, **30,** 7 (1956)
6. Mukhin, A. I., Ozerov, E. B., and Pontekorvo, B. M., *Zhur. Eksp. i Teoret. Fiz.*, **31,** 371 (1956)
7. (a) Low, F. E., *Phys. Rev.*, **97,** (1955); (b) Chew, G. F., and Low, F. E., *Phys. Rev.*, **101,** 1570 (1956); (Private communication)
8. Brueckner, K. A., *Phys. Rev.*, **86,** 106 (1952)
9. Castillejo, L., Dalitz, R. H., and Dyson, F. J., *Phys. Rev.*, **101,** 453 (1956)
10. Ashkin, J., Blaser, J. P., Feiner, F., and Stern, M. O., *Phys. Rev.*, **101,** 1149 (1956); *Phys. Rev.* **105,** 724 (1957)
11. (a) Anderson, H. L., and Glicksman, M., *Phys. Rev.*, **100,** 268 (1955); (b) Anderson, H. L., Davidon, W. C., Glicksman, M., and Kruse, U. E., *Phys. Rev.*, **100,** 279 (1955)
12. Anderson, H. L., Fermi, E., Martin, R., and Nagle, D. E., *Phys. Rev.*, **91,** 155 (1953)
13. (a) de Hoffmann, F., Metropolis, N., Alei, E. F., and Bethe, H. A., *Phys. Rev.*, **95,** 1586 (1954); (b) Anderson, H. L., and Metroplis, N., *Proc. 6th Ann. Rochester Conf on High Energy Physics*, Chap. 1, 19 (Interscience Publisher Inc., New York, N. Y., 1956)
14. Bethe, H. A., and de Hoffmann, F., *Mesons and Fields*, **2,** (Row Peterson and Company, 446 pp., White Plains, N. Y. 1955)
15. Orear, J., Jr., *Phys. Rev.*, **96,** 1417 (1954)
16. Ferrari, G., Ferretti, L., Gessaroli, R., Manaresi, E., Puppi, G., Quareni, G., Ranzi, A., and Stanghellini, A., *CERN Symposium Proc. (Geneva)*, **V2,** p. 230 (1956)
17. Taft, H., *Phys. Rev.*, **101,** 1116 (1956)
18. (a) Orear, J., *Phys.*, **96,** 176 (1954) (b) *Phys. Rev.*, **100,** 288 (1955)
19. Yang, C. N., (Private communication to E. Fermi)
20. (a) Minami, S., *Progr. Theoret. Phys.*, **11,** 213 (1954); (b) Hayakawa, S., Kawaguchi, M., and Minami, S., *Prog. Theoret. Phys.*, **11,** 332 (1954)
21. (a) Salam, A., *CERN Symposium Proc.* (Geneva), **V2,** p. 179 (1956); (b) Davidon, W. C. and Goldberger, M. L., *Phys. Rev.*, **104,** 1119 (1956); (c) Capps, R. N., and Takeda, G., *Phys. Rev.*, **103,** 1877 (1956); (d) Goldberger, M. L., *6th Ann. Rochester Conf. on High Energy Physics*, Chap. 1, 1 (Interscience Publisher, New York, N. Y., 1956)
22. Anderson, H. L., Davidon, W. C., Kruse, U. E., *Phys. Rev.*, **100,** 339 (1955)
23. Fermi, E., *Phys. Rev.*, **91,** 947 (1953)
24. (a) Ashkin, J. (Private communication); (b) Feld, B. T., (Private communication)
25. Cool, R., Piccioni, O., and Clark D., *Phys. Rev.*, **103,** 1082 (1956)
26. Leonard, S. J., and Stork, D. H., *Phys. Rev.* **93,** 568 (1954)
27. Bodansky, D., Sachs, A., and Steinberger, J., *Phys. Rev.*, **93,** 1367 (1954)
28. Perry, J. P., and Angell, C. E., *Phys. Rev.*, **91,** 1289 (1953)
29. Dyson, F. J., *Phys. Rev.*, **99,** 1037 (1955)

30. Takeda, G., *Phys. Rev.*, **100,** 440 (1955)
31. Walker, W. D., Hushfar, F., Shephard, W. D., *Phys. Rev.*, **104,** 526 (1956)
32. Lindenbaum, S. J., and Sternheimer, R. M., *Phys. Rev.* (In press)
33. Crew, J. E., Hill, R. D., and Lavatelli L., *Phys. Rev.* (In press)
34. (a) Barshay, S., *Phys. Rev.*, **103,** 1102 (1956); (b) Franklin, J., *Phys. Rev.*, **105,** 1101 (1957)
35. Karplus, R., and Ruderman, M. A., *Phys. Rev.*, **98,** 771 (1955)
36. (a) Goldberger, M. L., *Phys. Rev.*, **99,** 979; (b) Goldberger, M. L.,. Miyazawa, H., and Oehme, R., *Phys. Rev.*, **99,** 986 (1955)
37. Symanzik, K., *Phys. Rev.*, **105,** 743 (1957)
38. Bogoliubov, N. N., (Paper presented at the Intern. Conf. on Theoret. Phys. Seattle, Wash. (1956)
39. Haber-Schaim, U., *Phys. Rev.*, **104,** 1113 (1956)
40. (a) Bernardini, G., and Goldwasser, E. L., *Phys. Rev.*, **95,** 857 (1954); (b) Beneventano, M., Stoppini, G., Tau, L., and Bernardini, G., *CERN Symposium Proc. (Geneva)*, **V2,** p. 259 (1956)
41. (a) Puppi, G., and Stanghellini, A., *CERN Symposium Proc. (Geneva)*, **V2,** 182, (b) Puppi, G., (Private communication) (c) Chew, G. F., Private communication) (d) Goldberger, M. L., (Private communication) (e) Agodi, A., Cini, M., Vitale, B., (Private communication).
42. Ignatenko, A. E., Mukhin, A. I., Ozerov. E. B., and Pontekorvo, B. M., *Doklady Akad. Nauk. S.S.S.R.*, **103,** 209 (1955)
43. (a) Brueckner, K. A., *Phys. Rev.*, **89,** 834 (1953); (b) *Phys. Rev.*, **90,** 715 (1953); Tamm, I. E., Golfand, I. A., Zharkov, G. F., Poriskoia, L. V., and Feinberg, V. I., *Conf. on Quantum Electrodynamics and the Theory of Elementary Particles, U.S.S.R.* March 31, (1955)
44. Glauber, R. J., *Phys. Rev.*, **100,** 242 (1955)
45. (a) Rogers, K. C., and Lederman, L. M., *Phys. Rev.*, **105,** (1957); (b) Rockmore, R., *Phys. Rev.*, **105,** 256 (1957)
46. Ignatenko, A. E., Mukhin, A. I., Ozerov, E. B., and Pontekorvo, B. M., *Doklady Akad. Nauk., S.S.S.R.*, **103,** 395 (1955); *Rept. Inst. of Nuclear Problems, U.S.S.R. Acad. Sci.*, Moscow (1955)
47. (a) Serber, R., *Phys. Rev.*, **72,** 1114 (1947); (b) Fernbach, S., Serber, R., and Taylor, T. B., *Phys. Rev.*, **75,** 1382 (1949)
48. Sternheimer, R. M., *Phys. Rev.*, **101,** 384 (1956)
49. Abashian, A., Cool, R., and Cronin, J., *Bull. Am. Phys. Soc.*, [II], **1,** 350 (1956); *Phys. Rev.*, **104,** 855 (1956)
50. Hahn, B., Ravenhall, D. G., and Hofstadter, B., *Phys. Rev.*, **101,** 1131 (1956)
51. Williams, R. W., *CERN Symposium Proc. (Geneva)*, **V2,** 182 (1956); *Phys. Rev.*, **99,** 1387 (1955)
52. (a) Pevsner, A., Rainwater, J., Williams, R. E., and Lindenbaum, S. J., *Phys. Rev.*, **100,** 1419 (1955); (b) Pevsner, A., and Rainwater, J., *Phys. Rev.*, **100,** 1431 (1955)
53. (a) Williams, R. E., Rainwater, J., and Pevsner, A., *Phys. Rev.* **101,**, 412 (1956); (b) Williams, R. E., Baker, W. F., and Rainwater, J., *Phys. Rev.*, **104,** 1695 (1956)
54. Baker, W. F., *Scattering of 80 Mev π Mesons by Complex Nuclei* (Doctoral Thesis, Columbia University, New York, N. Y., March 1957)
55. Dzhelepov, V. P., Ivanov, V. G., Kozodaev, M. S., Osipenkov, V. T., Petrov, N. I., and Rusakov, V. A., *Rept. Inst. of Nuclear Problems, U. S.S.R. Acad. Sci.*, Moscow (1955)

56. Kozodaev, M. S., Sulaiev, R. M., Filippov, A. I., and Scherbakov, I. A., *RINP*, (USSR) (1955)
57. Mitin, N. A., and Grigoriev, E. L., *Doklady Akad. Nauk.* S.S.S.R., **103,** 210 (1955)
58. Ignatenko, A. E., *CERN Symposium Proc. (Geneva)*, **V2,** 313 (1956)
59. (a) Blau, M., and Oliver, A. R., *Phys. Rev.*, **102,** 489 (1956); (b) Blau, M., and Caulton, M., *Phys. Rev.*, **96,** 150 (1954)
60. (a) Feldman, D., *Proc. of 6th Ann. Rochester Conf. on High Energy Physics* Chap. 1, 1 (Interscience Publisher, New York, N. Y., (1956); (b) Wolfenstein, L., *Ann. Rev. Nuclear Sci.*, **6,** 43 (1957); (c) Signell, P. S., and Marshak, R. E., *Phys. Rev.* (In press); (d) Gammel, J. L., and Thaler, R. M., *Phys. Rev.* (In press)
61. (a) Smith, L. W., McReynolds, A. W., and Snow, G., *Phys. Rev.*, **97,** 1186 (1955); (b) Chen, F. F., Leavitt, C., and Shapiro, A. M., *Phys. Rev.*, **103,** 211 (1956)
62. Fowler, W. B. *et al.*, *Phys. Rev.*, **103,** 1472, 1479, 1484, 1489, (1956)
63. (a) Meshcheriakov, M. G., Neganov, B. S., Soroko, L. M., Vzorov, I. K., *Doklady Akad. Nauk.* S.S.S.R., **99,** 959 (1954); (b) Dzhelepov, V. P., Moskoloev, V. I., Medved., S. V., *Doklady Akad. Nauk.* S.S.S.R., **104,** 380 (1955); (c) Meshcheriakov, M. G., Bogochev, N. P., Leskin, G. A., Neganov, B. S., and Piskarev, E. V., *CERN Symposium Proc. (Geneva)*, **V2,** p. 125 (1956)
64. (a) Batson, A. P., Culwick, B., Riddiford, L., and Walker, J., *CERN Symposium Proc. (Geneva)*, **V2** p. 340 (1956); (b) Hughes, I. S., March, P. V., Muirhead, H., and Lock, W. O., *CERN Symposium Proc. (Geneva)*, **V2,** 344 (1956)
65. (a) Sutton, R. B., Fields, T. H., Fox J. G., Kane, J. A., Mott, W. E., and Stallwood, R. A., *Phys. Rev.*, **97,** 783 (1955); (b) Marshall, J., Marshall, L., and Nedzel, V. A., *Phys. Rev.*, **98,** 1513 (1955); (c) Kruse, U. E., Teem, J. M., and Ramsey, N. F., *Phys. Rev.*, **101,** 1079 (1956)
66. (a) Serber, R., and Rarita, W., *Phys. Rev.*, 99, 629(A) (1955); (b) Rarita, W., *Phys. Rev.*, **104,** 221 (1956)
67. Dzhelepov, V. P., Golovin, B. M., Kazarinov, I. M., and Semenov, M. M., *CERN Symposium Proc. (Geneva)*, **V2,** 115 (1956)
68. Coor, T., Hill, D. A., Hornyak, W., Smith, L., and Snow, G., *Phys. Rev.*, **98,** 1369 (1955)
69. Yuan, L. C. L., and Lindenbaum, S. J., *Phys. Rev.*, **103,** 404 (1956); *Phys. Rev.*, **93,** (1954)
70. (a) Fowler, E., Shutt, R. P., Thorndike, A. M., and Whittemore, W. L., *Phys. Rev.*, **95,** 1026 (1954); (b) Wallenmeyer, W. A., *Phys. Rev.*, **105,** 1058 (1957)
71. (a) Rosenfeld, A. H., *Phys. Rev.*, **96,** 139 (1954); (b) Merrison, A. W., *CERN Symposium Proc. (Geneva)*, **V2,** 239 (1956)
72. (a) Meshcheriakov, M. G., Neganov, B. S., *Doklady Akad. Nauk.* S.S.S.R., **100,** 677 (1955); (b) Meshcheriakov, M. G., Zrelov, V. P., Neganov, B. S., Vzorov, I. K., and Shabudin, A. F., *CERN Symposium Proc. (Geneva)*, **V2,** 347, 353, 357, (1956); (c) Mesh Kovshki, A. G., Pligin, Iu. S., Shalomov, Ia. Ia., and Shebanov, V. A., *CERN Symposium Proc. (Geneva)*, **V2,** p. 362 (1956); (d) Sidorov, V. M., *CERN Symposium Proc. (Geneva)* **V2,** 366 (1956); (e) Baiukov, Iu. D., Kozodaev, M. S., and Tiapkin, A. A., *CERN Symposium Proc. (Geneva)*, **V2,** p. 398 (1956)
73. (a) Brueckner, K. A., *Phys. Rev.*, **82,** 598 (1951); (b) Watson, K. M., and Brueckner, K. A., *Phys. Rev.* **83,** 1 (1951)

74. Alston, M. H., Crewe, A. V., Evans, W. H., and Von Gierke, G., *CERN Symposium Proc. (Geneva)*, **V2,** 334 (1956)
75. Lindenbaum, S. J., Sternheimer, R. M., *Phys. Rev.*, **105,** 1874 (1957)
76. (a) Peaslee, D. C., *Phys. Rev.*, **94,** 1085 (1954); (b) *Phys. Rev.*, **95,** 1580 (1954)
77. Kovacs, J. S., *Phys. Rev.*, **101,** 397 (1956)
78. Belenki, S. Z., and Nikishov, A. I., *Zhur. Eksp. i Teoret. Fiz.*, **28,** 744 (1955)
79. Preston, W. M., *Proc. 6th Ann. Rochester Conf.*, Sec. IV-47 (1956)
80. (a) Bernardini, G., Booth, E. T., and Lindenbaum, S. J., *Phys. Rev.*, **83,** 669 (1951); (b) *Phys. Rev.*, **88,** 1017 (1952); (c) Morrison, G. C., Muirhead, H., and Rosser, W. G. V., *Phil. Mag.*, **44,** 1326 (1953); (d) Goldberger, M. L., *Phys. Rev.*, **74,** 1269 (1948); (e) McManus, H., Sharp, W. T., and Gell-Mann, H., *Bull. Am. Phys. Soc.*, **28,** 20 (1953)
81. Wolfgang, R., Baker, E. W., Caretto, A. A., Cumming, J. B., Friedlander, G., and Hudis, J., *Phys. Rev.*, **103,** 394 (1956)
82. (a) Lock, W. O., March, P. V., Muirhead, H., and Rosser, W. G. V., *Proc. Roy. Soc. (London) A*, **230,** 215 (1955); Lock, W. O., March, P. V., and McKeaque, R., *Proc. Roy. Soc. (London) A*, **231,** 368
83. (a) Lock, W. O., and March, P. V., *Proc. Roy. Soc. (London), A*, **230,** 223 (1955); (b) McKeaque, *Proc. Roy. Soc. (London), A*, **236,** 104 (1956)
84. (a) Biller, W. F., *Univ. Calif. Radiation Lab. UCRL Report* 2067 (unpublished); (b) Vinogradov, A. P., Alimarin, I. P., Baranov, V. I., Lovrukhina, A. P., Baranova, T. V., Povlotskaya, F. I., Bragina, T. V., and Yakovlev, Yu. V., *Conf. Acad. Sci. U.S.S.R. Peaceful Uses of Atomic Energy, Moscow 1955, Session Div. Chem. Sci.*, 97; (c) Murin, A. N., Preobrazhensky, B. K., Yutlandov, I. A., and Yokimov, M. A., *Conf. Acad. Sci. U.S.S.R., Peaceful Uses of Atomic Energy, Moscow 1955, Session Div. of Chem. Sci.*, 160; (d) Steiner, N. M., and Jungerman, J. A., *Phys. Rev.*, **101,** 807 (1956)
85. Bivins, R., Metropolis, N., Storm, M., Turkevich, A., Miller, J. M., and Friedlander, G., *Bull. Am. Phys. Soc.* [II], **2,** 63 (1957)
86. (a) Nedzel, V. A., *Phys. Rev.*, **94,** 174 (1954) (b) Taylor, T. B., *Phys. Rev.*, **92,** 831 (1953)
87. Voss, R. G. P., and Wilson, R., *Proc. Roy. Soc. (London), A.*, **236,** 41 (1956); Woods, R. D., and Saxon, D., *Phys. Rev.*, **95,** 1279 (1954)
88. (a) Chen, F. F., Leavitt, C., Shapiro, A.M., *Phys. Rev.*, **99,** 857 (1955); (b) Richardson, R. E., Ball, W. P., Leith, C. E., Jr., and Moyer, B. J., *Phys. Rev.*, **86,** 29 (1952)
89. Margulies, R. S., *Bull. Am. Phys. Soc.*, **30,** 28 (1955)
90. Cini, M., and Fubini, S., *CERN Symposium Proc., (Geneva)*, **V2,** 171 (1956)
91. Batson, A. P., Culwick, B., and Piddiford, L. (Private communication)
92. Fermi, E., *Progr. Theoret. Phys. (Japan)*, **5,** 570 (1950); *Phys. Rev.*, **92,** 452 (1953); **93,** 1435 (1954)
93. Lepore, J. V., and Neumann, M., *Phys. Rev.*, **98,** 1484 (1955)